Journal of Archaeological Science: Reports 54 (2024) 104400

Contents lists available at ScienceDirect

Journal of Archaeological Science: Reports

journal homepage: www.elsevier.com/locate/jasrep

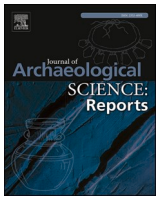

Clayey materials for traditional bricks production in North-Eastern Italy through a combined compositional study: From firing dynamics to provenance

Elena Mercedes Pérez-Monserrat [a,*], Laura Crespo-López [b], Giuseppe Cultrone [b], Paolo Mozzi [a], Lara Maritan [a]

[a] Department of Geosciences, University of Padua, Padua, Italy
[b] Department of Mineralogy and Petrology, Faculty of Sciences, University of Granada, Granada, Spain

ARTICLE INFO

Keywords:
XRPD and XRF techniques
Mg-content clays
High-temperature silicates
Experimental firing
Clays mixtures
Geochemical fingerprints

ABSTRACT

The compositional study of two main types of clayey materials outcropping nearby Padua (Veneto region, north-eastern Italy) and bricks used in historical constructions of the city is here addressed. Mineralogically, the clayey materials are illitic-chloritc clays, both non-carbonatic and carbonatic/highly-carbonatic clays, that chemically correspond to clays with important contents of silica and/or iron and of calcium and/or magnesium, respectively. Two main type of historic bricks were produced: i) one using mixtures of illitic/illitic-chloritic clays with abundant quartz and of carbonatic clays and firing temperatures between 950 and 1000 °C, and ii) a second one made out of illitic-chloritic clays non-carbonatic and fired around 850–900 °C. The comparative analysis between the mineralogical changes occurred in the clayey materials with increasing temperatures and the mineral assemblages detected in the studied bricks have provided evidences about the mixture of raw clays, that could be in turn compositionally similar to those analysed. The development of aluminium and magnesium-calcium silicates and/or magnesium silicates during the firing was fostered by mixing such base clays, giving rise to very durable and highly calcareous bricks. Whereas titanium and the trace elements zircon, vanadium, chromium and zinc may entail markers of provenance of illitic-chloritic clays quarried in the area, the strontium may represent a geochemical fingerprint for constraining supply areas of carbonatic clays. The compositional analysis carried out through the combined use of X-Ray Powder Diffraction (XRPD) and X-Ray Fluorescence Spectrometry (XRF) has provided data regarding to the composition and provenance of the starting clays as well as procedures and firing dynamics adopted for the manufacturing of the traditional bricks in the city of Padua from Roman Times to Renaissance.

1. Introduction

Earthen materials have been used in construction since ancient times, firstly sun-dried (adobe) and later fired (clay bricks). The worldwide use of fired bricks is mainly due to the abundance of clays on the earth's surface, a geo-resource relatively easy to be extracted, to give form and to transform into a ceramic product. Clay bricks build up heritage constructions and entail traditional materials meaningfully linked with cultural identities of peoples. Combined studies of local clayey deposits and traditional bricks of a given area provide valuable insights about the ancient technologies adopted for brick manufacturing (Pavia, 2006; Grifa et al., 2017; Dalkılıç and Nabikoğlu, 2017).

Large dimension bricks were used to build many Roman constructions and, after the fall of the Western Empire, brick production was properly reactivated in the ancient continent during the 12th century, when it was assumed by the Dutch (Campbell and Pryce, 2003). The 18-19th centuries marked the large-scale production and in the 20th century the reduction of the firing times or the production of lightweight bricks with high mechanical resistance were progressively achieved (Lourenço et al., 2010; Ramos et al., 2018). By the end of the last century, industry began to focus on sustainable brick production (Domínguez and Ullmann, 1996). In fact, eco-innovative solutions based on

* Corresponding author.
E-mail addresses: elenamercedes.perezmonserrat@unipd.it (E.M. Pérez-Monserrat), lcrespo@ugr.es (L. Crespo-López), cultrone@ugr.es (G. Cultrone), paolo.mozzi@unipd.it (P. Mozzi), lara.maritan@unipd.it (L. Maritan).

https://doi.org/10.1016/j.jasrep.2024.104400
Received 30 September 2023; Received in revised form 14 January 2024; Accepted 15 January 2024
Available online 1 February 2024

the reuse of waste products as additives have been researched since the last decades (Cultrone and Sebastian, 2009; Coletti et al., 2018; Coletti et al. (2023); Crespo et al., 2023). Nowadays, the most innovative technologies point towards the development of 3D printed bricks (Abdallah and Estévez, 2021; Sangiorgio et al., 2022).

Clays, mainly composed of silicates (including phyllosilicates) and/or carbonates, transform into a ceramic product by firing. During the firing process, the minerals present in the base clays undergo decomposition (their lattice breakdown) according their thermal stability, forming an amorphous phase enriched in silica that decreases with increasing temperature as newly mineral phases nucleate and/or growth (Rathossi and Pontikes, 2010). The firing of carbonatic clays between 700 and 1000 °C gives rise to Al-Ca silicates (such as gehlenite or anorthite), Mg-Ca silicates (such as diopside) and/or Mg-silicates (such as forsterite), accordingly with the calcite and dolomite contents in the starting clays (Cultrone et al., 2001; Trindade et al., 2009). These high-temperature mineral phases result from the reaction of the chemical elements made available from the phyllosilicates breakdown with other silicates (such as quartz), as well as with the lime and/or periclase derived from the decomposition of calcite and/or dolomite (Duminuco et al., 1996). In addition to the co-existence of relicts of the primary minerals with the firing phases, secondary or post-firing phases can be found in historic bricks. These phases were formed after firing, mainly from the transformation of the firing phases (both minerals and amorphous) and/or related to chemical processes occurred in the environs where the bricks were laid (Maritan, 2020; Pérez-Monserrat et al., 2022b).

From the mineralogical and chemical analysis of clayey deposits outcropping nearby Padua (Veneto region, north-eastern Italy) and of historic bricks used in the built heritage of the city, the primary aim of this research consists in performing the comparative study between the two types of materials. Besides, by the experimental firings to be carried out, an increasing knowledge of the firing dynamics of carbonatic clays with a significant presence of dolomite is expected to achieve.

1.1. Clayey deposits nearby Padua and the key role of bricks in the built heritage of the city

The province of Padua is located in the eastern Po Plain (Veneto region, north-eastern Italy) and it lies on the quaternary alluvial sediments of the Adige, Brenta and Bacchiglione rivers (Fig. 1a). The sand fraction of these deposits mainly comprises silicates (quartz, K-feldspars and plagioclase), carbonates (calcite and dolomite) as well as metamorphic and volcanic rock fragments. The clay fraction consists chiefly of clay minerals such as illite, chlorite, montmorillonite and kaolinite. Hematite, iron-manganese nodules, Ti-bearing minerals, apatite and zircon occur frequently as accessory minerals (Jobstraibitzer and Malesani, 1973). Clays with significant amounts of iron from the weathering of the nearby volcanic rocks, especially the trachyte of the Euganean Hills (Fig. 1b), and carbonatic clays related with the formation of the calcic pedogenic horizons, are extensively present in such deposits (Mozzi et al., 2003; Maritan, 2004; Cucato et al., 2008). The abundance of clayey deposits has conditioned the wide use of fired bricks as building material along history in the city, providing in turn cohesion and identity to the area and fostering a leadership ceramic industry in the region.

The territory of Padua has been occupied by human settlements since the Late Bronze Age (9-8th centuries BCE) and the municipium of *Patavium* was a strategic trade area during Roman Times, enhanced by its geographical centrality in the Veneto region and its nourished fluvial system. Between the 5th and 10th centuries, periods of depopulation and reactivation occurred in the city, starting the recovering of the area at the beginning of the 11th century. In the 12-13th centuries, during the Middle Ages, the expansion of the city was marked by a deep urban

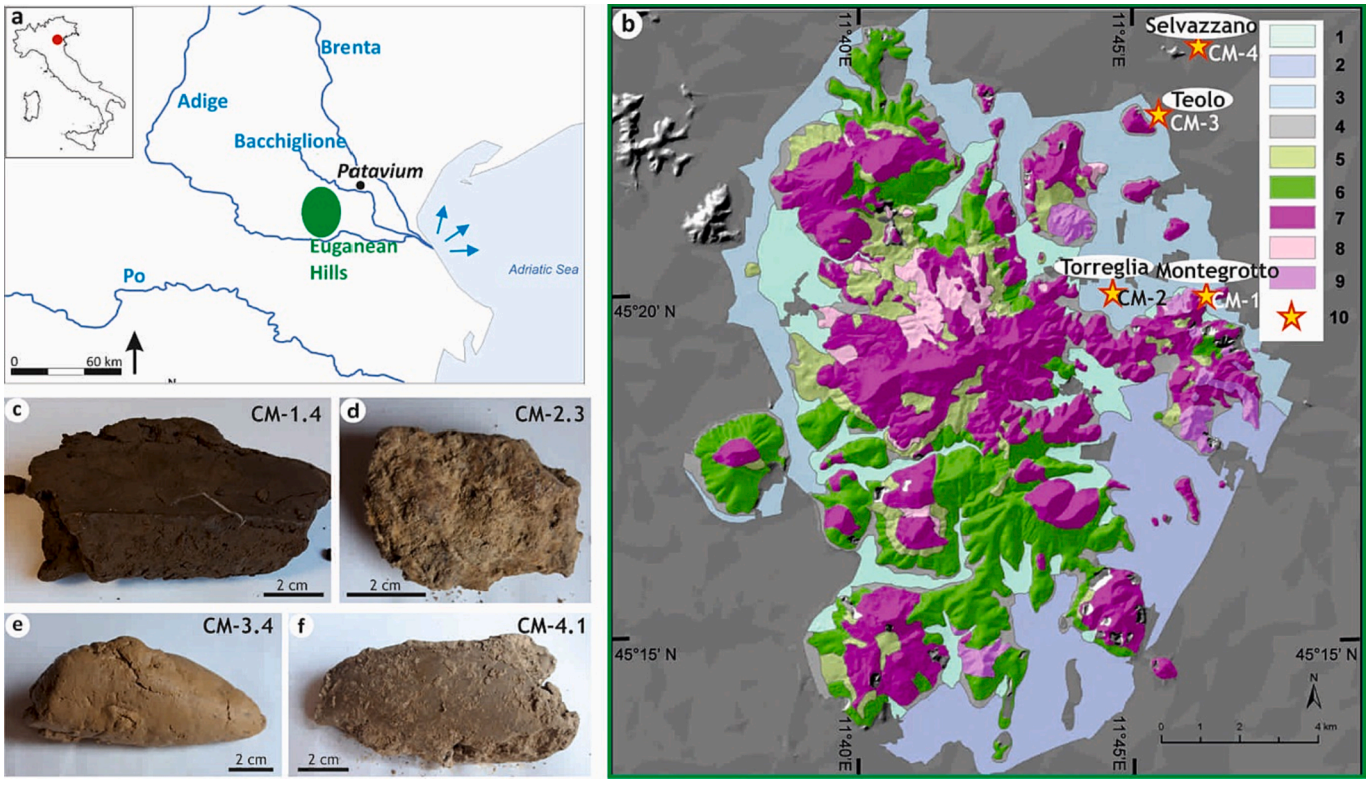

Fig. 1. (a) Location of Padua's province (red circle) in north-eastern Italy and the waterways of the main rivers flowing nearby Patavium at Roman times (from Germinario et al., 2018); (b) Simplified geological sketch map of the Euganean Hills (from Piccoli et al., 1981): 1. Fluvial deposits of local streams, 2. Fluvial deposits of the Adige River, 3. Fluvial deposits of the Brenta-Bacchiglione River, 4. Slope deposits, 5. Marl, 6. Limestone, 7. Rhyolite and trachyte, 8. Basalt, 9. Latite, 10. Sampling site; (c-f) Hand specimens of one of the clayey materials cored in each of the four boreholes.

awareness (Chavarría, 2011). Along the 14th century, a more stable reunification of the territory as well as an extraordinary cultural and artistic development were attained. At the beginning of the 15th century, Padua's territory was annexed to the Republic of Venice, starting from the Renaissance a new era of economic and cultural growth.

In Roman Times, many brick-making workshops arisen in the area (Bonetto, 2015), where the firing temperatures reached 900–1000 °C (Cagnana, 2000). Brick manufacturing ceased after the fall of the Western Empire and, to date, no data has been found about brick production in the city along the Late Antiquity. The reuse of Roman bricks was a very extensive practice during the 12-13th centuries (Chavarría, 2011). The reused bricks were normally cut to be fitted within the new fabrics (Causarano, 2019) and companies devoted to the recovery and sale of ancient building materials emerged (Calaon, 2015). The reuse practice ceased along the Middle Ages as the production of bricks was reactivated and new furnaces were built. The bricks that were then produced were smaller in size than the Roman ones and their production, dimension and trade were strictly controlled by the Municipality (Gloria, 1873). The most important brick work built in Padua under the Venetian Republic was the Renaissance Walls, a defensive system that provided a new urban design to the city (Mazzi et al., 2002).

Definitely, Padua's history is collected in the built heritage of the city, where the fired brick is entangled with peoples and shapes very emblematic constructions currently well-preserved. From Roman Times to Renaissance, the main technological modifications progressively accomplished for the brick manufacturing in the city were the production of bricks using a lesser content of carbonatic clays and the decrease of the firing temperatures (Pérez-Monserrat et al., 2021, 2022a, 2022b).

2. Materials and methods

2.1. Materials: Clayey materials (air/dried and fired) and historical bricks

2.1.1. Sampling

Two compositional types of clayey materials (CM) nearby the city of Padua were collected (Table 1 and Fig. 1c-1f): i) Fe-content colluvial deposits from weathering of trachyte rocks (CM-1), in Montegrotto Terme's locality, and ii) carbonatic alluvial sediments from the Brenta floodplain in three different locations, Torreglia (CM-2), Teolo (CM-3) and Selvazzano (CM-4) (Fig. 1b). The clay sediments were cored with a manual drilling designed for non-cemented materials and 2 to 4 core-like sediments ranging between 50 and 160 cm depth were taken in each borehole. Ten of the clayey materials cored were considered. Samples CM-1, CM-2.1, CM-3.4 and CM-4 were rather compacted, CM-1 shown dark nodules 1–2 mm in size and CM-3.4 had an important silty content (Fig. 1e); carbonate fragments were visible both in CM-2.3 (somehow friable) and in CM-3.2 and CM-3.3 (both highly friable).

38 well-preserved bricks from five historic constructions of the city of Padua were sampled. Diverse constructive typologies, built up during the Roman times, Late Antiquity, Middle Ages or Renaissance, were considered (Table 1 and Fig. 2). Fragments of historical bricks (HB) were taken from: i) the Basilica of Saint Justine (SJ, 5/6th to 16th centuries, 11 brick samples), comprising areas built in the 5-6th centuries (Late Antiquity) and in the 12-13th centuries of the Middle Ages as well as the Roman remains (1–3/4th centuries) still preserved under the basilica, ii) the Church of Saint Sophia (SS, 12th century, 5 samples), iii) the Eldery Tower (ET, 13th century, 2 brick samples), iv) the Tower of the Ancient Castle (AC, 14th century, 5 bricks) and v) the Renaissance Walls (RW,

Table 1
Clayey materials (CM) and historical bricks (HB) analysed.

CLAYEY MATERIALS (10 samples)								
Clayey sediments	**Sample**	**Site**	**Sample**	**Site**		**Sample**	**Site**	
Fe-content colluvial deposits. Weathering of trachyte rocks	CM-1.1 CM-1.3 CM-1.4	Montegrotto Terme Lat.: 45° 19′ 39'' N Long.: 11° 46′ 27'' E						
Carbonatic alluvial deposits Brenta's floodplain	CM-2.1 CM-2.3	Torreglia Lat.: 45° 20′ 06″N Long.: 11° 44′ 46'' E	CM-3.2 CM-3.3 CM-3.4	Teolo Lat.: 45° 22′ 41'' N Long.:11°45′ 04'' E		CM-4.1 CM-4.2	Selvazzano Lat.: 45° 23′ 12'' N Long.:11°46′35'' E	
HISTORIAL BRICKS (38 samples)								
Constructions	**Sample**	**Height***	**Facing**	**Sample**	**Height**	**Facing**	**Sample**	**Height**	**Facing**
Basilica of S. Justine (SJ), 5/6th to 16th centuries:								
- Roman remains, 1–3/4th	SJ-1	50	N	SJ-2	40	N	SJ-3	50	W
- Late Antiquity, 5-6th	SJ-4	120	SW	SJ-5	100	SW	SJ-6	70	E
- Middle Ages, 12-13th	SJ-7 SJ-10	130 280	E S	SJ-8 SJ-11	150 250	E S	SJ-9	170	E
Church of S. Sophia (SS), 12th century	SS-1 SS-4	10 20	E N	SS-2 SS-5	30 30	E N	SS-3	20	E
Eldery Tower (ET), 13th century	ET-1	20	N	ET-2	150	S			
Tower of the Ancient Castle (AC), 14th century	AC-1 AC-4	50 10	W W	AC-2 AC-5	50 20	W W	AC-3	30	S
Renaissance Walls (RW), 16th century:									
- Facing North	RW-1 RW-4	80 20	N N	RW-2	60	N	RW-3	50	N
Facing South	RW-5 RW-8	100 80	S W	RW-6	40	S	RW-7	100	S
Facing East	RW-9	150	E	RW-10	210	W	RW-11	60	E
Facing West	RW-12 RW-15	40 35	W E	RW-13	50	N	RW-14	25	W

*Height (in cm).

Fig. 2. Historical constructions selected and the location of some of the bricks collected.

16th century, 15 samples).

2.1.2. Samples preparation and experimental firing of the clayey materials

Water was added until the clayey materials attained the enough plasticity to be hand-kneaded and large lumps were placed in a 10 cm diameter plastic mould, then pressed in order to achieve discs about 3–4 cm thick. The discs were cut into four portions, that were experimentally fired at 700, 800, 900 or 1000 °C under oxidising atmosphere in an electric furnace equipped with an electronic controller. Firing was conducted as follow: heating was with a rate of 200 °C/h, soaking time of six hours and cooling according to the kiln drift (about nine hours). When preparing the brick samples, the outer areas of the fragments to be analysed were removed with a micro-drill, to eliminate surface deposits and/or contamination. Prior to the mineralogical and chemical analysis, the CM and HB samples were totally dried (at 100 °C for 24 h) and were reduced to powder in an agate mortar and then micronized (very fine powder, ≈10 μm) using a McCrone Micronising Mill (Bish and Reynolds, 1989).

2.2. Methods

Since compositionally different clays yield to different mineralogical changes during firing, the detection through XRPD of the mineral assemblages present in a ceramic product provides information about the mineralogical composition of the starting clays and of the firing conditions (Maritan et al., 2006). By the experimental firing of raw clays, the development of such changes with increasing temperatures and/or the reactions occurred when different base clays are mixed can be detected. As the chemical bulk composition of base clays remains almost the same after the firing, the general chemical composition of the used clayey materials can be stated by the XRF analysis of the ceramic product. When the compositional study of traditional bricks of a given area is addressed, especially important is the analysis of the minor oxides and of the trace elements (including rare earths). On the one side, such elements barely undergo any compositional changes during firing. On the other, these elements are associated to specific accessory minerals strongly related to the surrounding geology (Hein et al., 2004). Therefore, their variability and concentrations may constrain the provenance of the used geo-resources (clayey sediments) or, at least, may point out different supply areas.

The mineralogical composition of the clayey materials (both air-dried and fired at 700, 800, 900 and 1000 °C) and of the historical bricks was determined by means of a PANalytical X'Pert PRO diffractometer, operating in Bragg-Brentano reflection geometry. The PANalytical X'Pert HighScore Plus® software was used qualitatively to identify the mineral phases occurring in each sample. The semi-quantitative concentrations (in wt%) were estimated by the mass fractions of the identified phases using the Reference Intensity Ratio (RIR) values from the database selected for the qualitative identification (Wolff and Visser, 1964; Hubbard and Snyder, 1988).

The chemical composition of the 10 clayey materials (air-dried) and of the 38 historical bricks was determined by X-ray Fluorescence Spectrometry using a PANalytical Zetium compact spectrometer. Quantitative chemical analyses of major and minor oxides (SiO_2, TiO_2, Al_2O_3, Fe_2O_3, MnO, MgO, CaO, Na_2O, K_2O and P_2O_5 -in wt%-) and trace elements (S, Sc, V, Cr, Co, Ni, Cu, Zn, Ga, Rb, Sr, Y, Zr, Nb, Ba, La, Ce, Nd, Pb, Th and U -in ppm-), were carried out. A set of geological standards, analytically tested by the international scientific community (Govindaraju, 1994), was used for calibration following the internal instrumental precision proposed by Maritan et al. (2023). The values of P_2O_5 and S were not considered for the interpretation of the results, since they are chiefly related with the environs where the bricks were placed. Loss on ignition was gravimetrically determined as the weight loss recorded between 110 and 1000 °C.

3. Results and discussion

3.1. XRPD: Detecting the mineralogical composition

3.1.1. Clayey materials (air-dried and fired) and historical bricks

The mineral phases identified by XRPD and their semi-quantitative concentrations estimated by RIR in the CM and HB samples are shown in Tables 2 and 3, respectively. The air-dried CM were mainly composed of quartz, K-feldspars, albite, phyllosilicates (chlorite and illite-like phase) and/or carbonates (dolomite and calcite). CM-1 samples display the highest contents of silicates (quartz, feldspars and phyllosilicates) and in CM-2, CM-3 and CM-4 important amounts of carbonates were detected (note the significative presence of dolomite). Mineralogically, CM-1 and CM-2 can be classified as illitic-chloritic clays with a significant quartz content (CM-2 also as carbonatic clays), CM-3 as illitic-chloritic (with a lower chlorite content) and highly carbonatic clays and CM-4 as illitic-chloritic and highly carbonatic clays.

The mineralogical changes occurred by the experimental firing of the

Table 2
Mineralogical assemblages detected by XRPD analysis in clayey materials (CM), air-dried and fired, and RIR semi-quantitative analysis (in wt%). Relict minerals: Chl (chlorite), Ilt (illite-like phase), Ab (albite), Qz (quartz), Kfs (K-feldspar), Cal (calcite) and Dol (dolomite); firing phases: Gh (gehlenite), Lrn (larnite), Ran (rankinite), An (anorthite), Di (diopside), Tob (Tobermorite), Per (periclase), Por (portlandite) and Hem (hematite). Abbreviations from Warr (2021).

CLAYEY MATERIALS																
Air-dried		**Chl**	**Ilt**	**Qz**	**Kfs**	**Ab**	**Dol**	**Cal**	**Mineralogical classification of the clayey materials**								
CM-1.1		5	22	35	19	19	–	–	Illitic-chloritc clays								
CM-1.3		13	30	28	15	14	–	–	(with important quartz content)								
CM-1.4		16	34	24	9	17	–	–									
CM-2.1		9	17	34	21	12	3	4	Illitic-chloritc and carbonatic clays								
CM-2.3		13	15	28	11	13	8	12	(with important quartz content)								
CM-3.2		4	26	21	9	15	9	16	Illitic-chloritc and highly carbonatic clays								
CM-3.3		3	24	17	7	10	19	20	(with a lower chlorite content)								
CM-3.4		3	11	16	2	10	34	24									
CM-4.1		14	22	29	3	3	17	12	Illitic-chloritic and highly carbonatic clays								
CM-4.2		19	26	17	6	8	14	10									
Fired	**T (°C)**	**Chl**	**Ilt**	**Qz**	**Kfs**	**Ab**	**Dol**	**Cal**	**Gh**	**Lrn**	**Ran**	**An**	**Di**	**Tob**	**Per**	**Por**	**Hem**
CM-1.1	700	–	28	39	17	16	–	–	–	–	–	–	–	–	–	–	–
	800	–	19	40	18	21	–	–	–	–	–	–	–	–	–	–	2
	900	–	1	42	26	27	–	–	–	–	–	–	–	–	–	–	4
	1000	–	–	43	25	25	–	–	–	–	–	–	–	–	–	–	7
CM-1.3	700	7	28	33	14	18	–	–	–	–	–	–	–	–	–	–	–
	800	–	22	35	21	19	–	–	–	–	–	–	–	–	–	–	3
	900	–	3	36	28	27	–	–	–	–	–	–	–	–	–	–	6
	1000	–	–	38	27	25	–	–	–	–	–	–	–	–	–	–	10
CM-1.4	700	8	29	30	15	18	–	–	–	–	–	–	–	–	–	–	–
	800	–	20	34	21	22	–	–	–	–	–	–	–	–	–	–	3
	900	–	2	40	26	27	–	–	–	–	–	–	–	–	–	–	5
	1000	–	–	41	25	25	–	–	–	–	–	–	–	–	–	–	9
CM-2.1	700	4	21	38	17	18	–	2	–	–	–	–	–	–	–	–	–
	800	–	17	36	20	21	–	–	2	4	–	–	–	–	–	–	–
	900	–	2	30	21	22	–	–	6	10	–	6	3	–	–	–	–
	1000	–	–	27	17	20	–	–	12	8	–	9	7	–	–	–	–
CM-2.3	700	2	14	32	12	21	–	14	–	5	–	–	–	–	–	–	–
	800	–	1	28	23	17	–	10	5	16	–	–	–	–	–	–	–
	900	–	2	27	21	–	–	3	12	20	–	13	2	–	–	–	–
	1000	–	–	23	14	–	–	–	20	18	–	18	7	–	–	–	–
CM-3.2	700	2	17	24	12	14	7	17	–	2	–	–	–	–	3	2	–
	800	–	6	22	14	16	–	14	–	10	–	–	–	–	8	10	–
	900	–	–	21	12	13	–	4	3	12	–	8	–	8	11	8	–
	1000	–	–	17	9	10	–	–	4	15	–	12	–	9	15	9	–
CM-3.3	700	1	16	22	3	13	9	21	–	6	–	–	–	–	5	4	–
	800	–	4	20	–	12	–	16	–	17	–	–	–	–	16	15	–
	900	–	–	19	–	–	–	5	6	19	–	15	–	8	17	11	–
	1000	–	–	15	–	–	–	–	2	22	–	19	–	12	19	11	–
CM-3.4	700	2	9	24	–	11	12	26	–	5	–	–	–	–	7	4	–
	800	–	7	23	–	11	–	21	–	14	–	–	–	–	13	11	–
	900	–	–	21	–	–	–	8	5	17	–	13	–	11	17	8	–
	1000	–	–	9	–	–	–	–	4	27	–	17	–	10	24	9	–
CM-4.1	700	8	18	32	8	12	8	14	–	–	–	–	–	–	–	–	–
	800	–	15	31	14	14	–	4	4	–	18	–	–	–	–	–	–
	900	–	11	26	14	–	–	–	16	–	15	14	4	–	–	–	–
	1000	–	–	16	15	–	–	–	24	–	–	17	28	–	–	–	–
CM-4.2	700	10	30	23	9	8	8	12	–	–	–	–	–	–	–	–	–
	800	–	28	25	8	9	–	6	8	–	16	–	–	–	–	–	–
	900	–	15	26	9		–	–	17	–	15	12	6	–	–	–	–
	1000	–		20	10		–	–	23	–	5	19	23	–	–	–	–

Table 3
Mineralogical assemblages detected by XRPD analysis in historical bricks (HB) and RIR semi-quantitative analysis (in wt%). Relict minerals: Ilt (illite-like phase), Ab (albite), Qz (quartz), Kfs (K-feldspar), Cal (calcite) and Dol (dolomite); firing phases: Gh (gehlenite), Di (diopside), An (anortithe), Fo (forsterite) and Hem (hematite); secondary phases: Cal (calcite) and Arg (aragonite). Abbreviations from Warr (2021).

HISTORICAL BRICKS

Type 1. Important formation of Al- and Mg-Ca silicates and/or Mg-silicates (high-T phases)

Sub-type 1a. Di >> An, Fo nucleation and low Qz amounts
Base clays: illitic clays with important Qz-content and carbonatic clays. Firing T: circa 1000 °C

	Ilt	Qz	Kfs	Ab	Gh	Di	An	Fo	Hem	Cal	Arg
HB-RW-2	–	5	–	–	5	55	24	5	–	5	–
HB-RW-15	–	–	–	–	2	53	32	5	–	8	–
HB-SS-3	–	9	–	–	6	52	23	–	–	11	–
HB-SJ-2	–	10	15	–	–	52	21	3	–	–	–
HB-SJ-4	–	5	–	–	5	52	28	–	–	10	–
HB-SJ-6	–	3	–	–	–	50	40	–	–	7	–
HB-AC-1	–	4	–	–	2	49	34	3	–	7	–
HB-SJ-9	–	12	–	–	–	49	30	5	–	–	–
HB-ET-1	–	6	–	–	–	48	40	6	–	–	–
HB-RW-5	–	9	–	–	4	45	31	10	–	–	–
HB-RW-11	–	17	–	–	–	41	29	–	–	13	–
HB-RW-3	–	15	–	–	2	39	39	4	–	–	–
HB-SJ-8	–	6	22	–	3	39	21	3	–	6	–
HB-SS-2	–	12	15	–	–	38	36	–	–	–	
HB-SJ-1	–	15	11	–	3	37	20	–	–	14	–
HB-SJ-3	–	14	9	–	–	37	39	–	–	–	–
HB-RW-13	–	16	–	–	6	35	32	–	–	–	–

Sub-type 1b. Di > An or An > Di and higher Qz amounts
Base clays: illitic clays with important Qz-content and carbonatic clays. Firing T: 950–1000 °C

	Ilt	Qz	Kfs	Ab	Gh	Di	An	Fo	Hem	Cal	Arg
HB-RW-8	–	25	–	–	7	33	25	–	–	10	–
HB-SJ-11	–	13	23	–	–	32	26	–	–	6	–
HB-SJ-5	–	17	19	–	7	30	21	–	–	6	–
HB-SJ-10	–	14	25	–	–	29	31	–	1	–	–
HB-AC-5	–	16	25	–	–	29	29	–	–	–	–
HB-ET-2	–	17	12	–	5	26	37	–	–	3	–
HB-RW-6	–	17	23	–	6	25	23	–	–	5	–
HB-AC-4	6	18	26	–	–	25	17	–	–	8	–
HB-SJ-7	–	17	–	–	9	25	17	–	–	9	23
HB-SS-4	–	15	20	–	–	23	42	–	–	–	–
HB-SS-1	–	10	–	–	11	20	32	–	–	15	12
HB-AC-3	–	16	34	–	–	20	21	–	2	6	–

Type 2. Important presence of relict minerals and/or Hem formation (high-T phase)
Base clays: illitic-chloritic clays with variable Qz-content. Firing T: 850–900 °C

	Ilt	Qz	Kfs	Ab	Gh	Di	An	Fo	Hem	Cal	Arg
HB-RW-12	4	21	37	30	4	–	–	–	2	2	–
HB-AC-2	–	22	38	33	–	–	–	–	3	3	–
HB-SS-5	–	30	36	27	–	–	–	–	3	2	–
HB-RW-1	8	32	27	25	–	–	–	–	2	6	–
HB-RW-10	2	39	29	15	–	–	–	–	1	14	–
HB-RW-14	–	46	28	15	–	–	–	–	–	11	–
HB-RW-7	–	51	19	24	–	–	–	–	3	3	–
Miscellaneous	**Ilt**	**Qz**	**Kfs**	**Ab**	**Ak**	**Di**	**An**	**Fo**	**Hem**	**Cal**	**Arg**
HB-RW-4	–	27	30	18	3	10	–	–	–	3	9
HB-RW-9	–	17	25	–	–	–	49	–	5	3	–

clayey materials are also included in Table 2 and the diffraction patterns of four clayey materials (CM-1.1, CM-2.3, CM-3.4 and CM-4.1) -one sample for each borehole- with increasing temperatures are shown in Fig. 3. Chlorite was still detected after 700 °C, since it decomposes around 750 °C (Maritan et al., 2006). Illite-like phase is progressively reduced till 800 °C and it almost disappeared after 900 °C, as the total breakdown of the dehydroxylated phase occurs between 850 and 950 °C (Aras, 2004). Although K-feldspars progressively decreasing since they are involved in high-temperature phases nucleation (Riccardi et al., 1999), it should be taken into consideration the sanidine formation with increasing temperature, from microcline transformation (Elias and Cultrone, 2019) and/or with the potassium provided by illite decomposition (Trindade et al., 2009). In the carbonatic clays, dolomite concentration drastically decreased at 700 °C and disappeared completely after 800 °C, as its decomposition into calcite and periclase begins circa 500 °C (Rodríguez-Navarro et al., 2012) and ends around 750–800 °C (Maritan et al., 2006). Calcite is still remained in traces at 900 °C (Fig. 3b and 3c), chiefly due to its high content in the starting clays, since the thermal decomposition of calcite is completed about 800–850 °C (Iordanidis et al., 2009).

The absence or presence of carbonates, as well as their grain-size, in the base clays largely determined the mineral phases nucleated and/or growth with increasing temperatures. In CM-1 samples (illitic-chloritic clays non-carbonatic), hematite started developing from 800 °C and increased after heating at 900 °C (Fig. 3a), since its formation is enhanced by the iron oxide released from the breakdown of chlorite and well-crystallized hematite is a significant component only over 900 °C (Vedder and Wilkings, 1969; Trindade et al., 2009). When carbonates

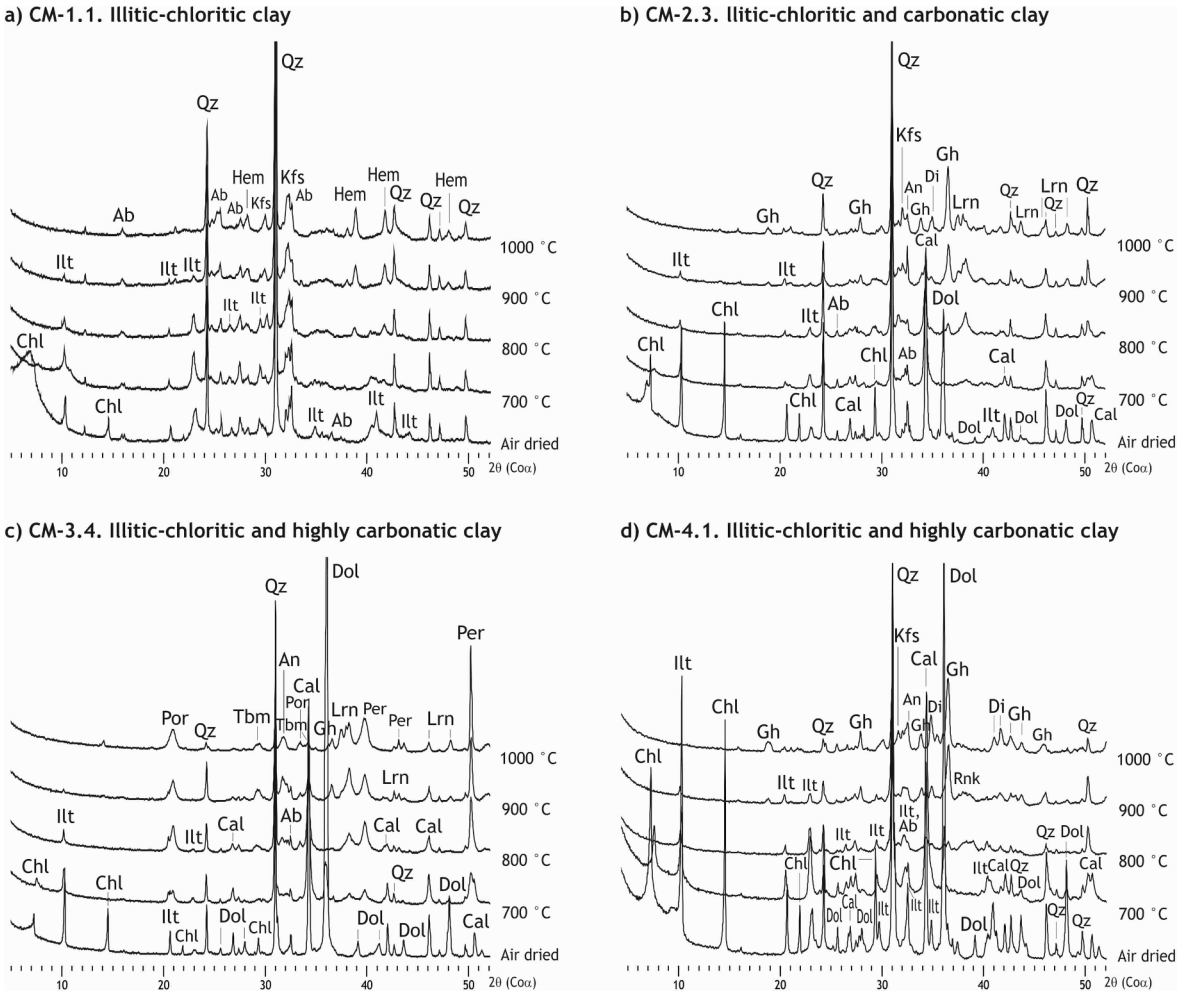

Fig. 3. XRPD patterns of clayey materials (CM) with increasing temperature. Relict minerals: Chl (chlorite), Ilt (illite-like phase), Ab (albite), Qz (quartz), Kfs (K-feldspar), Cal (calcite) and Dol (dolomite); firing phases: Gh (gehlenite), Di (diopside), An (anortithe), Fo (forsterite), Hem (hematite), Por (portlandite), Tbm (tobermorite) and Lrn (larnite); secondary phases: Cal (calcite) and Arg (aragonite). Abbreviations from Warr (2021).

were present, the following is observed: i) gehlenite development after 800 °C, as its formation starts at about 800–850 °C (Cultrone et al., 2001), and the emerging nucleation of diopside from 900 °C in CM-2.3 and CM-4.1 (Fig. 3b and 3d); ii) early transformation of albite to anorthite after 900 °C in CM-2.3, CM-3.4 and CM-4.1 (Fig. 3b, 3c and 3d); iii) larnite nucleation from 700 °C in CM-2.3 and CM-3.4, increasing progressively until after 900 °C or even after 1000 °C (Fig. 3b and 3c); and iv) portlandite and periclase formation from 700 °C in CM-3.4, both more developed the higher the temperatures were (Fig. 3c).

Because of the low quantities of phyllosilicates and the extremely high content of carbonates in sample CM-3.4, very abundant lime and periclase remained unreacted. As the reactivity of lime is higher than that of periclase (Webb, 1952), the former promptly reacted with the few oxides available whereas the later remained almost unchanged, increasingly accumulated and even sintered. Due to the very high content of calcite in this sample, abundant lime might be still free after firing, that reacted with the environ humidity and formed portlandite (post-firing process). Special attention should be paid if mineralogically similar clays to this sample CM-3.4 were used, because portlandite reacts with the atmospheric CO_2 and forms secondary calcite, that may provoke the cracking of the ceramic product (Jain et al., 1976), defect known as lime blowing. Besides, the periclase sintering would prevent its reaction to form new silicates (Rodríguez-Navarro et al., 2012), high-temperature mineral phases that improve the mechanical resistance of the ceramics (Celik et al., 2019). It would be necessary to mix it with clays highly rich in phyllosilicates, in order to enhance Mg- and Al-Ca silicates and/or Mg-silicates nucleation during the firing and, therefore, almost no lime and periclase remain unreacted.

Concerning to the historical bricks, two main types were distinguished on the basis of the mineral assemblages (Table 3): i) Type 1, characterized by high contents of diopside and anorthite, some also with gehlenite and/or forsterite, and ii) Type 2, bricks with hematite. Type 1 bricks comprised in turn bricks in which diopside quantities were in general much higher than those of anorthite (sub-type 1a), and bricks with somehow similar concentrations of both mineral phases (sub-type 1b). Accordingly, lower or higher contents of quartz and feldspars were estimated, respectively, as both primary minerals were also consumed to form the high-temperature phases.

3.1.2. Production technologies: Firing dynamics and mixture of the base clays

The mineral assemblages and their estimated content in type 1 bricks point out that illitic clays with important quantities of quartz and carbonates (calcite and dolomite) were used. Since high anorthite and diopside concentrations denote firing temperatures exceeding 950 °C (Cultrone et al., 2001; Daghmehchi et al., 2016), the firing might reach around 1000 °C. The noticeably higher contents of diopside in bricks belonging to sub-type 1a indicate higher temperatures (nearer 1000 °C) than those reached during the firing of sub-type 1b bricks (nearer 950 °C).

Base clays compositionally similar to CM-2 or CM-4 might be used to produce type 1 bricks, as both contains phyllosilicates and carbonates. However, the comparative analysis between the mineralogical changes occurred in the clayey materials with increasing temperatures and the mineralogical assemblages detected in these type 1 bricks, provides evidences about the mixture of clays, a well-known practice since ancient times to improve the clay workability and the properties of the final ceramic product (Kingery and Vandiever, 1986). Hence, the following was observed: i) the well-developed gehlenite in CM-2.3 and CM-4.1 from 900 °C (Fig. 3b and 3d) decreased in bricks, mostly at expenses of diopside nucleation as stated elsewhere (Flores et al., 1999); ii) much more significative was the development of anorthite in bricks than in clays, giving rise to the almost complete transformation of albite to anorthite through the progressive Ca-enrichment of the former with increasing temperature (Cultrone et al., 2014), note that no albite was detected in type 1 bricks; and iii) periclase was not detected in bricks, as reacted to form diopside and/or forsterite.

It should be pointed out that the base clays, rather than illitic clays, might be illitic-chloritic clays, although almost no hematite was detected by XRPD, that should have formed from the iron provided after chlorite breakdown at the high temperatures that were reached (950–1000 °C). When the firing of carbonatic clays gives rise to the formation of Al-Ca silicates and/or Mg-Ca silicates, it should be considered that iron is entrapped within the structure of such mineral phases, hence hematite nucleation is inhibited (Klaarenbeek, 1961).

Hence, concerning to the production of type 1 bricks, the mixing of illitic/illitic-chloritic clays with important quartz contents and of carbonatic clays fired at 950–1000 °C might provide the suitable chemical stability by enhancing the development of Al- and Mg-Ca silicates and/or Mg-silicates and, therefore, almost no reactive oxides remained free after the firing. In any case, considering the high calcite content of the carbonatic clays that were used to produce this type of bricks, salt could be added to the mixtures and/or the bricks might be soaked in water in order to reduce the risk of lime blowing. That is, sodium chloride in very low concentrations fosters the reactions that yield the newly formed silicates (Laird and Worchester, 1956; Elias and Cultrone, 2019), and by submerging the bricks in water just after the firing, the free lime still available precipitates as calcite in the water surface and/or within the porosity of the bricks (Saenz et al., 2019). Another possibility could be that the carbonates in the used clays had a lower grain size, so that the reaction responsible of the Al-, Ca- and Mg-silicates nucleation were promoted with respect clays with larger carbonates where lime and portlandite tend to develop.

Regarding to type 2 bricks, both the detection of hematite and the absence of Al- and Mg-Ca silicates suggest that non-carbonatic illitic-chloritic clays were used. As illite-like phase is occasionally present in some bricks and the low concentrations detected of hematite point out its early nucleation, the firing temperatures might be about 850–900 °C. The base clays used were mineralogical similar to samples CM-1, being the iron mainly supplied by chlorite (Fe-bearing phyllosilicate).

The calcite detected in type 1 bricks should correspond mainly with a secondary phase, since at the high temperatures reached (950–1000 °C) calcite decarbonation might be completed. However, due to the important calcite content in the base clays, some calcite could be remained. In type 2 bricks (fired at 850–900 °C), the calcite detected may be also secondary; if it corresponded with remains of primary calcite not decomposed, more gehlenite should have been formed but low concentrations were slighted detected (Table 3). In any case, the grain size of calcite should be considered and the assignment of primary or secondary calcite should be confirmed by microscopic and microstructural observations (Fabbri et al., 2014; Maritan et al., 2021).

3.2. XRF: Detecting the chemical composition

3.2.1. Clayey materials (air-dried) and historical bricks

Based on the plotting of the compositional data in the ternary diagrams SiO_2-Al_2O_3-CaO and CaO-Fe_2O_3-MgO (Fig. 4), the CM range from clays with important silica and iron oxide contents (CM-1 and CM-2.1) to clays with significant amounts of calcium oxide (CM-3.3 and CM-3.4). All the bricks were plotted within such area of the diagrams and many of them were grouped in the carbonate compositional area, with variable quantities of silica and calcium oxide and a rather even alumina content (Fig. 4a). When the iron concentrations were considered, the data result more scattered (Fig. 4b), remaining as well many bricks clustered (with similar variation ranges in Ca, Fe and Mg).

The data distribution in both ternary diagrams points out likewise that many of the bricks were most probably produced from mixed clays with similar chemical compositions than those of the studied clayey materials. It is interesting to note that: i) the clustered bricks comprised construction materials from buildings dated to the Late Antiquity, Middle Ages and Renaissance, ii) the two samples with the highest calcium oxide concentration, plotted joint to CM-2.3 (Fig. 4a), corresponded with Roman bricks, ii) almost all the bricks from the Tower of the Ancient Castell (14th century) were found to have different calcium and/or iron content than those from the other constructions (Fig. 4b).

The chemical analysis of the 10 CM (air-dried) and of the 38 HB is shown in Table 4 (major and minor oxides) and Table 5 (trace elements). Regarding to CM, the highest contents of silica, alumina and iron oxide in CM-1 are in concordance with the highest concentrations of quartz, feldspars (K-feldspars and albite) and Fe-bearing phyllosilicates (chlorite), respectively. Besides, low amounts in alkaline-earth metals were detected (CaO + MgO $\approx$ 3 %). The MnO and TiO_2 values (generally higher than in CM-2, CM-3 and CM-4) are mainly related with the iron-manganese nodules and Ti-bearing accessory minerals commonly present in the quaternary sediments of Padua's territory (Jobstraibitzer and Malesani, 1973).

The high values of calcium and magnesium oxides in clays CM-2.3, CM-3 and CM-4.1 confirm the important presence of calcite and dolomite detected by XRPD, justifying in turn the high loss of ignition observed (LOI $>$ 18 %). CM-3.3, CM-3.4 and CM-4.1 were the richest in magnesia, supporting the highest dolomite concentrations. The maximum K_2O/Na_2O ratios in CM-1.3, CM-1.4 and CM-4 were in concordance with the important illite content estimated by RIR (Table 2). From a chemical point of view, CM-1 samples were mainly clays with significant amounts of silica and Fe-bearing clay minerals (high SiO_2 and moderately high Fe_2O_3 values), and CM-2.3, CM-3 and CM-4.1 were calcium and magnesium clays (with high/very high CaO and/or MgO quantities).

Concerning to the historical bricks, the average of silica detected is almost the same for sub-types 1a and 1b ($\approx$ 45 %), but the quartz concentrations were generally lower in the former (Table 3). This is because the silica quantities determined by XRF is forming part of the chemical composition both of relicts of quartz and K-feldspars and of the newly silicates nucleated during the firing (the same occurred with the alumina content).

The higher magnesia quantities determined in sub-type 1a bricks (average = 6.75 %) than in sub-type 1b, were chiefly related with the higher concentrations of diopside and forsterite. Although the higher calcium oxide amounts also detected in sub-type 1a (18 % versus 16.4 %) may largely corresponds with the higher amount of calcium silicates developed during the firing, it must be also considered the calcite (formed probably as secondary phase). The chemical composition of type 1 bricks indicates that they were made out of clays with important contents of silica, clay minerals and carbonates, supporting the mixture of two main compositionally different base clays, chemically similar in turn to the clayey materials analysed.

Type 2 bricks were richer in silica, alumina and iron oxide than type 1. These oxides mainly formed part of the minerals originally present in the base clays, that were largely preserved during the firing (except illite). The higher iron oxide values (6.2 % versus $\approx$ 5.4 %) are mostly related to the hematite developed as a firing phase. Since no calcium silicates were formed, just low concentrations of gehlenite (sample HB-

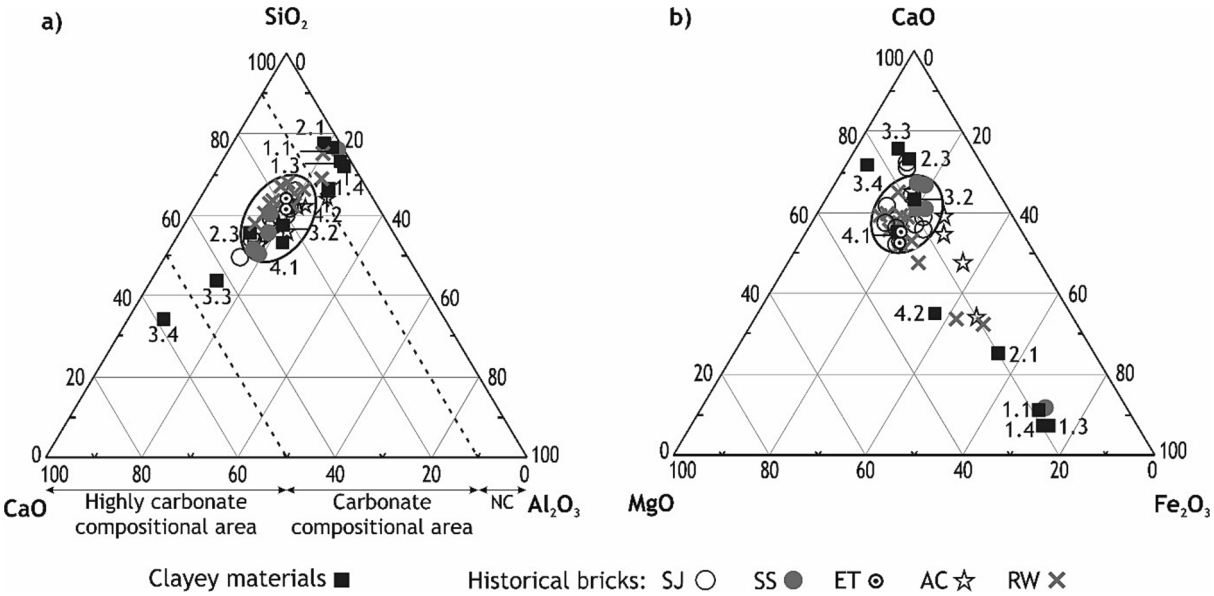

Fig. 4. Plotting of the chemical composition of clayey materials and historical bricks in the ternary diagrams SiO_2-Al_2O_3-CaO and CaO-Fe_2O_3-MgO. Abbreviations: SJ (Basilica of Saint Justine, 5/6-16th centuries), SS (Church of Saint Sophia, 12th century), ET (Eldery Tower, 13th century), AC (Tower of the Ancient Castle, 14th century and RW (Renaissance Walls, 16th century). NC: Non-carbonate compositional area.

RW-12), the calcium oxide concentrations determined may support that the calcite detected chiefly corresponds with secondary calcite. The chemical data point out the use of base clays with an important silica and clay mineral content and abundant K-feldspars, similar in composition to the CM-1 samples but richer in silica and magnesia and poorer in iron and titanium. At least three chemically different type of clays -with silica amounts under 50 %, around 50–52 % and about 60–62 % (Table 4)- were probably used for manufacturing the type 2 bricks.

When all the chemical data of both clays materials and historical bricks are considered, it emerges and interesting picture. In the score and loading plots of the principal component analysis (PCA) comprising the major and minor oxides and the trace elements (Fig. 5), the clayey materials range in compositions between the highest silica, alumina and iron content terms (CM-1.1 and CM-1.3) and the richest calcium and magnesium members (CM-3.3 and CM-3.4). Almost all the clayey materials plot between negative values of PC1 and PC2 and positive of PC1 and negative of PC2, while the bricks span all the diagram. CM-1 are richer in all the trace elements analysed, overall in Zr, V, Cr, Zn and Ba (high values were also determined in CM-2.1 and CM-4.2). CM-2.3, CM-3 and CM-4.1 shown in general significantly lower concentrations of trace elements, except in Rb, Sr and Ba (Table 5).

According to the loading plots, type 1 bricks shown a high scattered distribution, although some trends are observed (Fig. 5 and Table 5): i) three bricks from Saint Justine (SJ) -just one corresponding to a Roman brick- plot the nearest to the maximum component weights of CaO and MgO, and two plot jointly and with a significative Sr-content (HB-SJ-31 and 33, with 152 and 191 ppm); ii) three samples from Santa Sophia (SS) were especially rich in Sr (HB-SS-21, 22 and 23, with 220, 210 and 390 ppm); iii) despite of the high scattering shown by the bricks of the Tower of the Ancient Castell (AC), as observed in the ternary diagram of Fig. 4b, the majority were plotted at positive values of PC1 and PC2 and present important concentrations of Sr (HB-AC-16, 210 ppm), Rb (HB-AC-19, 180 ppm), Th (HB-AC-18, 16 ppm) and/or Ba (HB-AC-17, 560 ppm); and iv) the plotting of the bricks from the Renaissance Walls comprises both the positive and negative values of PC1 and PC2.

If, certainly, the more brick sampled from the Renaissance Walls should be considered, this last observation may suggest that during the 16th century areas previously quarried were still active and/or that the reuse of Roman bricks was in practice in the city of Padua when large dimension brick works were built. Significantly high contents of Sr (>200 ppm) were detected in some bricks (note that the highest Sr values determined in the CM samples were 151 ppm). In some of these bricks, high or extremely high quantities of Cr, Co, Cu, Zn and/or Rb were also determined.

Almost all bricks belonging to type 2 and the two miscellaneous bricks plot at positive values of PC1 and negative of PC2 and at negative values of PC1 and PC2. Most of them are rich or highly rich in Si, Fe and Al, as well as in Ti, Zr and Mn. Magnesium oxide forms mainly part of the illite relics still preserved after the firing, and the calcium contents chiefly correspond with the secondary calcite that might be formed in such type 2 bricks.

3.2.2. Production technologies: Mixture and provenance of the base clays

The high scattering of the loading plots of type 1 bricks is chiefly related with the use of mixtures of clays with important amounts of silica and/or iron and of clays with significant calcium and/or magnesium contents, chemically equivalent to CM-1 and CM-2/CM-3/CM-4 samples, respectively. Such scattering is also related to the different chemical compositions of the mixtures that were made. Thus, considering the opposite directions marked by the component weights of CaO and MgO to the left side, and of SiO_2 and TiO_2 to the right, the further towards the midpoint were the plots, the more similar were the proportions of the clays in the mixtures. No clays mixture procedure seems that were carried out for the manufacturing of type 2 bricks, that were produced by using clays compositionally similar to CM-1 type.

Some of the trace elements determined, overall the concentrations detected and keeping in mind the mixing of clays, may entail geochemical fingerprints when dealing with the provenance of the clayey materials used for brick manufacturing in the city of Padua. High values of Zr, V, Cr and Zn point out the use of clays compositionally similar to CM-1, corresponding with the nearby Fe-content colluvial deposits from weathering of trachyte rocks, and high concentrations of Rb and Sr the use of clays compositionally similar to CM-2/CM-3/CM-4. Exceptionally high quantities of Sr detected in some type 1 bricks suggest the use of carbonatic clays from specific areas. On the basis of the concentrations of trace elements, the greater or lesser quantity of illitic clays used in the mixtures could be estimated, since such elements are largely hosted by the illite-like mineral phase.

Table 4
Major and minor oxides (in wt%) of clayey materials (CM, air-dried) and historical bricks (HB) determined by XRF analysis.

CLAYEY MATERIALS													
	SiO_2	**Al_2O_3**	**Si/Al**	**K/Na**	**Fe_2O_3**	**MnO**	**MgO**	**CaO**	**Na_2O**	**K_2O**	**TiO_2**	**LOI**	**Total**
CM-1.1	59.2	16.2	3.65	2.02	8.93	0.24	2.30	1.34	1.24	2.51	1.96	5.74	99.93
CM-1.3	56.0	19.7	2.84	4.30	8.84	0.13	2.33	0.91	0.77	3.31	1.40	6.25	99.79
CM-1.4	57.0	19.5	2.92	4.37	8.46	0.08	2.32	0.92	0.76	3.32	1.30	6.08	99.95
CM-2.1	62.2	15.4	4.04	2.31	5.59	0.10	2.00	2.56	1.27	2.93	0.87	6.95	99.97
CM-2.3	37.7	9.9	3.81	2.40	3.38	0.04	3.95	20.2	0.77	1.85	0.54	21.5	99.98
CM-3.2	39.3	13.7	2.87	3.95	4.40	0.06	4.35	15.1	0.78	3.08	0.53	18.1	99.46
CM-3.3	27.1	8.5	3.19	3.22	2.93	0.04	5.30	26.1	0.54	1.74	0.40	26.9	99.61
CM-3.4	17.7	3.92	4.52	2.88	1.71	0.03	10.1	30.6	0.32	0.92	0.30	34.4	99.98
CM-4.1	33.2	14.1	2.35	4.69	5.08	0.08	7.13	15.3	0.58	2.72	0.55	21.0	99.82
CM-4.2	48.0	18.6	2.58	4.65	6.08	0.08	4.67	5.80	0.81	3.77	0.67	11.4	99.96
HISTORICAL BRICKS													
Type 1													
Sub-type 1a	**SiO_2**	**Al_2O_3**	**Si/Al**	**K/Na**	**Fe_2O_3**	**MnO**	**MgO**	**CaO**	**Na_2O**	**K_2O**	**TiO_2**	**LOI**	**Total**
HB-RW-2	43.6	11.2	3.89	1.94	4.54	0.09	9.59	20.9	1.05	2.04	0.86	4.85	98.96
HB-RW-15	43.5	15.0	2.90	1.15	5.64	0.10	7.99	17.8	1.51	1.73	0.74	5.35	99.67
HB-SS-3	41.1	13.7	3.00	2.48	6.18	0.11	5.87	19.2	1.23	3.05	0.61	8.37	99.70
HB-SJ-2	47.3	14.0	3.38	0.76	5.21	0.09	7.54	16.9	1.91	1.46	0.71	9.3	104.6
HB-SJ-4	36.7	11.2	3.28	1.44	4.11	0.07	5.39	25.6	1.21	1.74	0.51	13.3	99.98
HB-SJ-6	44.4	14.3	3.10	1.09	4.79	0.08	5.19	18.5	1.93	2.10	0.55	7.10	100.0
HB-AC-1	39.6	13.0	3.05	0.64	5.74	0.10	6.03	22.2	1.94	1.25	0.61	9.13	99.82
HB-SJ-9	49.3	15.0	3.29	1.78	5.51	0.09	7.71	14.7	1.35	2.40	0.74	2.51	99.54
HB-ET-1	49.0	15.5	3.16	1.86	5.83	0.11	7.64	15.0	1.39	2.58	0.74	1.53	99.54
HB-RW-5	42.8	14.4	2.97	2.37	5.42	0.10	7.32	17.3	1.09	2.58	0.67	8.04	99.94
HB-RW-11	46.7	11.3	4.13	2.03	4.59	0.08	7.57	15.5	1.10	2.23	0.83	9.81	99.96
HB-RW-3	48.7	15.9	3.06	2.30	5.61	0.10	7.08	13.9	1.28	2.94	0.66	3.24	99.61
HB-SJ-8	45.8	12.9	3.55	0.79	4.66	0.08	8.57	18.3	1.78	1.41	0.69	5.31	99.91
HB-SS-2	47.1	12.6	3.74	2.14	6.27	0.11	5.65	18.4	1.45	3.10	0.66	3.73	99.80
HB-SJ-1	40.1	11.4	3.52	2.36	4.05	0.06	5.11	22.4	1.04	2.45	0.53	12.8	100.1
HB-SJ-3	55.0	15.6	3.53	1.48	5.29	0.08	4.54	12.6	1.80	2.67	0.65	1.06	99.38
HB-RW-13	46.0	11.8	3.90	1.16	3.98	0.07	5.92	18.5	1.52	1.77	0.64	9.52	99.97
Average	**45.1**	**13.5**	**3.34**	**1.52**	**5.14**	**0.09**	**6.75**	**18.1**	**1.45**	**2.21**	**0.67**	**6.76**	**100.0**
Sub-type 1b	**SiO_2**	**Al_2O_3**	**Si/Al**	**K/Na**	**Fe_2O_3**	**MnO**	**MgO**	**CaO**	**Na_2O**	**K_2O**	**TiO_2**	**LOI**	**Total**
HB-RW-8	47.28	11.67	4.05	2.04	4.04	0.07	7.09	16.58	0.98	2.00	0.67	4.43	95.00
HB-SJ-11	46.31	14.36	3.22	2.69	5.00	0.08	5.06	13.68	1.32	3.55	0.52	5.92	95.95
HB-SJ-5	46.65	15.08	3.09	2.44	5.44	0.09	4.63	15.43	1.24	3.02	0.63	6.95	99.36
HB-SJ-10	50.84	15.10	3.37	2.51	5.49	0.09	7.23	14.55	1.21	3.04	0.71	1.71	100.2
HB-AC-5	50.20	17.13	2.93	3.15	7.08	0.10	4.03	13.54	1.26	3.97	0.74	8.61	106.9
HB-ET-2	50.54	14.21	3.56	2.29	5.01	0.08	6.68	14.42	1.08	2.47	0.73	4.52	99.95
HB-RW-6	49.42	13.22	3.74	2.09	4.83	0.09	6.42	16.50	1.01	2.11	0.65	7.39	101.9
HB-AC-4	42.74	16.85	2.54	2.37	7.39	0.12	4.14	16.99	1.43	3.39	0.70	5.40	99.66
HB-SJ-7	36.58	11.34	3.23	2.75	4.23	0.08	8.06	20.05	0.92	2.53	0.60	14.8	99.40
HB-SS-4	35.46	11.46	3.09	5.95	5.20	0.08	4.84	20.72	0.59	3.51	0.62	16.1	98.88
HB-SS-1	39.22	13.65	2.87	2.26	6.22	0.09	4.71	23.21	1.16	2.62	0.58	8.16	99.76
HB-AC-3	46.93	17.35	2.70	2.80	8.48	0.13	3.76	11.25	1.43	4.01	0.92	3.11	99.54
Average	**45.18**	**14.29**	**3.16**	**2.65**	**5.70**	**0.09**	**5.55**	**16.41**	**1.14**	**3.02**	**0.67**	**7.26**	**99.70**
Type 2	**SiO_2**	**Al_2O_3**	**Si/Al**	**K/Na**	**Fe_2O_3**	**MnO**	**MgO**	**CaO**	**Na_2O**	**K_2O**	**TiO_2**	**LOI**	**Total**
HB-RW-12	52.7	16.5	3.19	3.17	5.93	0.10	5.57	10.6	0.92	2.92	0.82	3.74	99.98
HB-AC-2	48.6	20.2	2.41	5.65	9.86	0.10	4.24	7.38	0.77	4.35	1.03	2.73	99.67
HB-SS-5	62.9	18.8	3.35	3.25	7.40	0.10	1.75	1.20	1.39	4.52	0.89	0.79	99.79
HB-RW-1	50.2	14.7	3.41	2.91	5.56	0.10	5.53	12.2	0.81	2.36	0.74	1.56	93.92
HB-RW-10	50.5	11.7	4.32	2.56	4.31	0.07	4.93	13.3	1.02	2.61	0.77	10.7	99.93
HB-RW-14	52.5	12.5	4.20	2.46	4.36	0.07	5.43	12.1	0.97	2.39	0.71	8.81	99.96
HB-RW-7	62.4	16.5	3.78	2.88	6.07	0.08	2.44	4.11	1.20	3.46	0.75	2.38	99.47
Average	**54.2**	**15.8**	**3.43**	**3.20**	**6.21**	**0.09**	**4.27**	**8.70**	**1.01**	**3.23**	**0.82**	**4.38**	**98.96**
Miscellaneous	**SiO_2**	**Al_2O_3**	**S/Al**	**K/Na**	**Fe_2O_3**	**MnO**	**MgO**	**CaO**	**Na_2O**	**K_2O**	**TiO_2**	**LOI**	**Total**
HB-RW-4	47.00	15.37	3.06	3.78	5.92	0.09	5.92	13.0	0.87	3.29	0.68	8.03	100.3
HB-RW-9	55.2	18.33	3.01	2.22	8.07	0.10	4.72	6.56	1.43	3.17	1.12	1.01	99.98

LOI: Loss on ignition.

4. Conclusions

Clayey materials compositionally similar to those analysed, corresponding with illitic-chloritic clays -both non-carbonatic with important quartz content and carbonatic/highly carbonatic (with important amounts of calcite and dolomite)- were traditionally used for brick manufacturing in the city of Padua. The mixture of both different compositional types of starting clays was an extensive production procedure, that enhanced the development of high-temperature silicates during the firing. By firing between 950 and 1000 °C such mixtures, very durable and highly calcareous bricks were produced. Bricks made out illitic-chloritic clays and fired around 850–900 °C were likewise

Table 5
Chemical composition of trace elements (in ppm) of clayey materials (CM, air-dried) and historical bricks (HB) determined by XRF analysis.

CLAYEY MATERIALS																				
	Zr	**Sc**	**V**	**Cr**	**Co**	**Ni**	**Cu**	**Zn**	**Ga**	**Rb**	**Sr**	**Y**	**Nb**	**Sn**	**Ba**	**La**	**Ce**	**Nd**	**Pb**	**Th**	**U**
CM-1.1	357	14	165	150	35	73	30	100	20	114	151	33	39	4	600	62	132	51	30	12	4
CM-1.3	267	17	148	122	19	66	34	126	24	155	109	33	27	4	597	57	112	51	34	14	3
CM-1.4	236	17	143	113	14	62	33	123	23	152	94	30	23	4	568	53	93	44	31	12	3
CM-2.1	254	13	95	88	13	37	31	117	17	141	79	31	19	5	549	49	89	39	52	13	2
CM-2.3	156	1	62	66	6	22	17	69	11	83	114	19	9	2	408	36	59	25	24	7	2
CM-3.2	125	9	75	63	10	26	23	88	17	129	108	28	10	4	552	35	75	35	44	11	2
CM-3.3	107	2	55	49	8	19	14	57	10	72	118	17	6	3	367	30	52	21	23	7	2
CM-3.4	75	2	38	32	6	12	10	32	4	32	105	9	4	2	152	22	26	12	11	3	2
CM-4.1	112	9	96	82	14	38	24	84	17	122	93	27	11	3	488	39	78	32	27	12	3
CM-4.2	161	17	109	91	15	41	27	119	22	180	89	35	13	5	643	48	93	40	43	15	3
HISTORICAL BRICKS																					
Type 1																					
Sub-type 1a	**Zr**	**Sc**	**V**	**Cr**	**Co**	**Ni**	**Cu**	**Zn**	**Ga**	**Rb**	**Sr**	**Y**	**Nb**	**Sn**	**Ba**	**La**	**Ce**	**Nd**	**Pb**	**Th**	**U**
HB-RW-2	203	5	82	118	78	43	28	80	13	126	308	25	16	4	402	45	70	32	26	9	3
HB-RW-15	153	10	78	104	18	52	30	96	18	194	204	31	14	5	549	43	82	39	33	12	3
HB-SS-3	190	18	72	73	12	29	40	66	13	180	390	24	11	8	520	44	77	35	47	16	4
HB-SJ-2	175	7	84	88	16	38	31	92	17	143	140	29	13	5	488	43	84	35	24	12	3
HB-SJ-4	127	1	75	68	12	32	24	79	13	111	252	23	9	2	424	35	71	28	7	10	3
HB-SJ-6	130	7	81	77	15	36	32	106	18	171	191	27	10	4	516	46	74	27	17	12	3
HB-AC-1	190	21	78	72	13	31	30	67	13	220	210	22	11	7	470	47	76	33	16	13	3
HB-SJ-9	173	10	90	93	16	43	34	98	18	139	144	31	14	4	489	44	88	45	46	12	3
HB-ET-1	176	10	72	107	29	47	39	105	19	166	163	33	15	6	526	48	91	44	37	13	4
HB-RW-5	146	10	84	87	20	54	31	95	17	164	171	30	13	4	494	45	85	41	33	11	3
HB-RW-11	174	5	74	77	13	37	21	78	12	103	176	23	14	4	350	36	62	32	31	8	2
HB-RW-3	163	12	79	84	18	40	31	99	19	152	156	32	13	4	555	51	91	39	35	14	3
HB-SJ-8	161	6	75	84	14	37	25	97	15	123	152	27	12	39	412	37	81	32	37	11	3
HB-SS-2	190	17	80	71	11	27	35	68	13	180	210	24	12	6	530	42	88	36	15	13	4
HB-SJ-1	138	1	65	59	11	25	23	84	13	95	246	23	9	3	433	38	70	28	6	10	3
HB-SJ-3	142	12	82	91	15	35	29	107	19	148	147	30	12	5	555	45	89	35	39	14	3
HB-RW-13	165	4	60	67	11	27	35	75	13	123	174	24	10	3	397	37	67	28	29	9	3
Average	**164**	**9**	**77**	**84**	**19**	**37**	**30**	**88**	**15**	**149**	**202**	**27**	**12**	**7**	**477**	**43**	**79**	**35**	**28**	**12**	**3**
Sub-type 1b	**Zr**	**Sc**	**V**	**Cr**	**Co**	**Ni**	**Cu**	**Zn**	**Ga**	**Rb**	**Sr**	**Y**	**Nb**	**Sn**	**Ba**	**La**	**Ce**	**Nd**	**Pb**	**Th**	**U**
HB-RW-8	155	4	76	57	11	29	19	70	13	86	120	22	11	1	380	35	62	28	27	8	2
HB-SJ-11	153	10	64	86	14	36	25	100	18	142	204	28	11	5	569	46	77	35	46	12	3
HB-SJ-5	160	11	80	88	14	41	30	307	18	146	196	30	12	5	596	50	88	35	67	13	3
HB-SJ-10	200	18	78	89	15	33	39	82	15	160	150	28	13	7	560	50	87	38	40	15	3
HB-AC-5	190	10	91	93	24	40	33	93	18	133	130	30	14	5	489	56	89	37	29	12	3
HB-ET-2	181	10	87	85	14	38	32	100	17	123	289	29	14	4	512	41	80	38	33	12	3
HB-RW-6	161	6	85	67	14	36	30	87	15	119	157	26	12	4	451	39	70	32	46	10	2
HB-AC-4	180	20	81	91	18	35	48	100	17	180	200	28	13	9	630	54	98	41	43	17	3
HB-SJ-7	138	3	67	70	13	35	33	92	13	108	187	23	11	7	405	30	58	27	37	8	2
HB-SS-4	190	15	72	52	12	23	26	50	10	91	240	20	10	6	380	35	60	25	25	11	3
HB-SS-1	170	22	79	72	12	30	35	70	14	180	220	24	11	8	580	46	82	37	21	15	4
HB-AC-3	240	18	87	150	18	44	79	160	17	180	240	31	15	9	650	49	97	41	42	16	4
Average	**177**	**12**	**79**	**83**	**15**	**35**	**36**	**109**	**15**	**137**	**194**	**27**	**12**	**6**	**517**	**44**	**79**	**35**	**38**	**12**	**3**
Type 2	**Zr**	**Sc**	**V**	**Cr**	**Co**	**Ni**	**Cu**	**Zn**	**Ga**	**Rb**	**Sr**	**Y**	**Nb**	**Sn**	**Ba**	**La**	**Ce**	**Nd**	**Pb**	**Th**	**U**
HB-RW-12	201	13	92	93	17	44	31	102	20	114	141	33	15	5	583	45	102	41	36	14	2
HB-AC-2	200	19	130	190	24	66	59	130	21	160	170	35	20	9	560	67	110	52	45	18	5
HB-SS-5	260	12	95	76	12	25	45	78	16	180	70	28	15	8	510	48	81	37	42	14	3
HB-RW-1	158	11	88	81	16	43	28	97	17	82	258	29	14	4	524	44	76	31	37	11	3
HB-RW-10	177	6	81	67	13	33	21	71	15	95	167	22	12	3	492	38	64	28	26	9	2
HB-RW-14	189	9	67	65	14	30	21	76	13	81	139	24	12	4	433	33	70	33	28	9	2
HB-RW-7	232	13	78	92	14	37	29	97	19	147	116	30	13	4	580	43	85	42	40	12	2
Average	**202**	**12**	**90**	**95**	**16**	**40**	**33**	**93**	**17**	**123**	**152**	**29**	**14**	**5**	**526**	**45**	**84**	**38**	**36**	**12**	**3**
Miscellaneous	**Zr**	**Sc**	**V**	**Cr**	**Co**	**Ni**	**Cu**	**Zn**	**Ga**	**Rb**	**Sr**	**Y**	**Nb**	**Sn**	**Ba**	**La**	**Ce**	**Nd**	**Pb**	**Th**	**U**
HB-RW-4	183	11	98	77	16	42	28	92	18	121	155	30	14	4	563	43	86	37	31	12	3
HB-RW-9	190	17	139	131	28	95	49	138	22	139	187	33	22	5	643	51	94	41	70	12	4

produced.

During more than fifteen centuries, from Roman Times to Renaissance, common extraction areas might be exploited. Titanium and the trace elements Zr, V, Cr and Zn entail markers of provenance of Fe-content illitic-chloritc clays quarried in the area (from the colluvial deposits from the weathering of the nearby volcanic rocks), and the Sr may represent an optimal geochemical fingerprint for constraining specific supply areas of carbonatic clays from the widely present alluvial deposits around the city.

The comparative analysis between local clayey deposits and traditional bricks through the combined use of XRPD and XRF techniques, provides significant data regarding to the production technologies adopted. Procedures such as the mixture of compositional different base clays and the firing and post-firing dynamics must be taken into consideration when interpreting the data, that may be complemented through of a broader multi-analytical study.

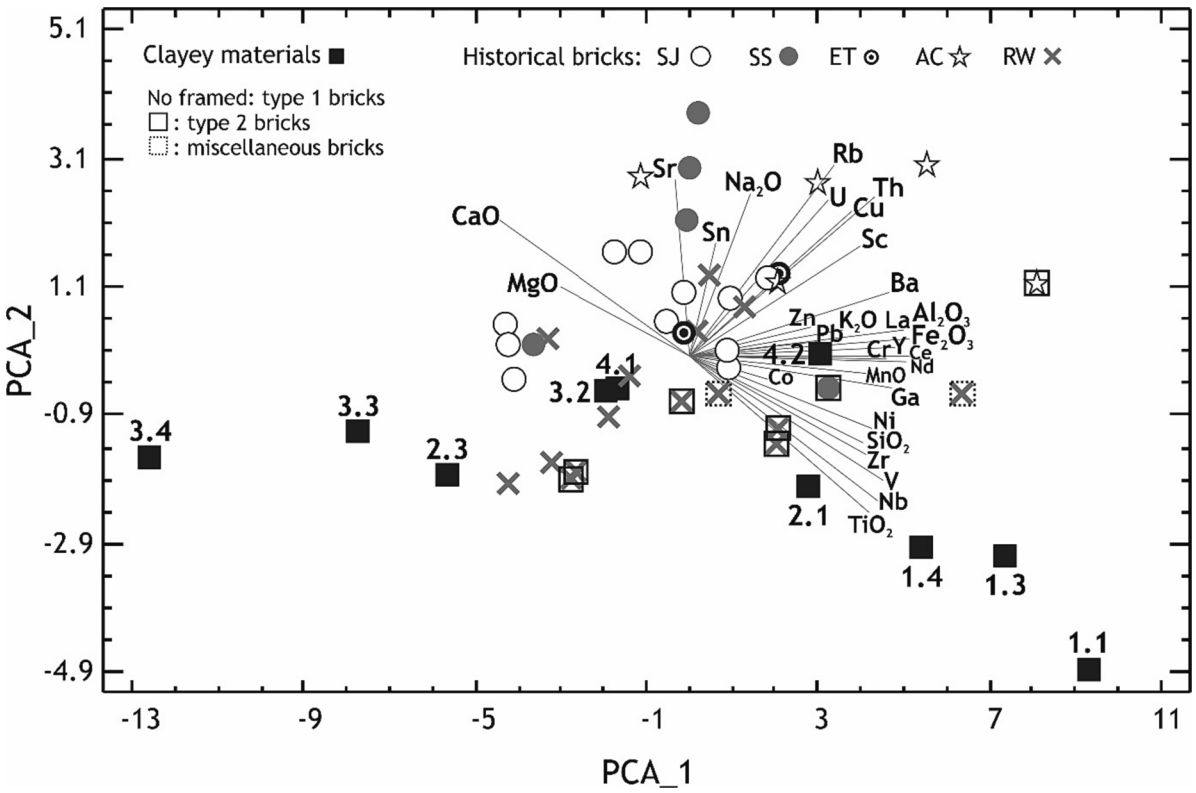

Fig. 5. Score and loading plots of PC1 and PC2, representing 53% and 10% of total variance, respectively, obtained by PCA of chemical data of the 10 clayey materials and the 38 historical bricks. Abbreviations: SJ (Basilica of Saint Justine, 5/6-16th centuries), SS (Church of Saint Sophia, 12th century), ET (Elderly Tower, 13th century), AC (Tower of the Ancient Castle, 14th century), and RW (Renaissance Walls, 16th century).

New insights about the mineralogical changes occurred during the firing of carbonatic clays with high dolomite contents have been provided. From the understanding of the mineralogical changes occurring with the experimental firing, some issues concerning to the potential suitability of local clayey materials for the regional ceramic industry has been tackled.

CRediT authorship contribution statement

Elena Mercedes Pérez-Monserrat: Conceptualization, Methodology, Investigation, Writing – original draft, Supervision. **Laura Crespo-López:** Investigation, Methodology, Writing – review & editing. **Giuseppe Cultrone:** Formal analysis, Investigation, Methodology, Resources. **Paolo Mozzi:** Data curation, Software, Writing – review & editing. **Lara Maritan:** Investigation, Methodology, Writing – review & editing.

Declaration of competing interest

The authors declare that they have no known competing financial interests or personal relationships that could have appeared to influence the work reported in this paper.

Data availability

No data was used for the research described in the article.

Acknowledgements

This work was supported by the European Union's Horizon 2020 Research and Innovation Programme under the Marie Sklodowska-Curie Individual Fellowship (grant agreement No 836122) and by the Research Group of the Junta de Andalucía, Spain (RNM179). The authors appreciate the facilities provided by the X-Ray Powder Diffractometry Laboratory of the Department of Geosciences of the University of Padua (Italy) and by the X-Ray Fluorescence Service of the Scientific Instrumentation Centre of the University of Granada (Spain). The sampling authorizations given by the Saint Justine Benedictine Abbey, the Surveillance Department of Venice's metropolitan area and Belluno, Padua and Treviso provinces, the City Hall of Padua and the National Institute of Astrophysics Astronomical Observatory of Padua are gratefully acknowledged. The authors thank the helpful assistance of Giulio Pagnoni (Saint Justine's abbot), Elisa Pagan (City Hall of Padua), Marie-Ange Causarano (Department of Cultural Heritage of the University of Padua) and Stefano Tuzzato during the sampling operations. Special thanks are given to Marco Favero (Department of Geosciences of the University of Padua) and Isabel Moreno (Scientific Instrumentation Centre of the University of Granada). The authors would like also to thank the suggestions provided by the anonymous reviewers.

References

Abdallah, Y.K., Estévez, A.T., 2021. 3D-Printed biodigital clay bricks. Biomimetics 6 (4), 59. https://doi.org/10.3390/biomimetics6040059.

Aras, A., 2004. The change of phase composition in kaolinite- and illite-rich clay-based ceramic bodies. Appl. Clay Sci. 24, 257–269. https://doi.org/10.1016/j.clay.2003.08.012.

Bish, D.L., Reynolds, R.C., 1989. Modern Powder Diffraction. In: Bish, D.L., Post, J.E. (Eds.), Reviews in Mineralogy & Geochemistry. De Gruyter, Berlin, Germany, Boston, MA, USA, pp. 73–100.

Bonetto, J., 2015. Diffusione e uso del mattone cotto nella Cisalpina romana tra ellenizzazione e romanizzazione. Archeologia Dell'architettura XX 105–113.

Cagnana, A., 2000. Archeologia dei materiali da costruzione. SAP Società Archeologica S. r.l, Mantova.

Calaon, D., 2015. Tecniche edilizie, materiali da costruzione e società in laguna tra VI e XI secolo, leggere gli spolia nel contesto archeologico, in: Centanni, M., Sperti, L. (Eds.), Atti del Convegno Internazionale Pietre di Venezia spolia in se spolia in re. Roma, pp. 85–111.

Campbell, J.W.P., Price, W., 2003. Brick. A World History. Thames and Hudson, London.

Causarano, M.A., 2019. Il reimpiego dei laterizi romani nell'edilizia medievale di Padova, in: E. Bukowiecki, E., Pizzo, A., Volpe, R. (Eds.), Proceedings III Workshop Internacional laterizio, demolire, riciclare, reinventare: la lunga vita e l'eredità del laterizio romano nella storia dell'architettura. Roma, pp. 109–114.
Çelik, A., Kadir, S., Kapur, S., Zorlu, K., Akça, E., Akşit, I., Cebeci, Z., 2019. The effect of high temperature minerals and microstructure on the compressive strength of bricks. Appl. Clay Sci. 169, 91–101. https://doi.org/10.1016/j.clay.2018.11.020.
Chavarría, A., 2011. Percezione e dato archeologico sull'architettura medievale a Padova in età comunale. Archeologia Dell'architettura XV 151–162.
Coletti, C., Maritan, L., Cultrone, G., Dalconi, M.C., Hein, A., Molina, E., Mazzoli, C., 2018. Recycling trachyte waste from the quarry to the brick industry: Effects on physical and mechanical properties, and durability of new bricks. Constr. Build. Mater. 166, 792–807. https://doi.org/10.1016/j.conbuildmat.2018.01.158.
Coletti, C., Bragié, E., Dalconi, M.C., Mazzoli, C., Hein, A., Maritan, L., 2023. A new brick-type using grape stalks waste from wine production as pore-agent. Open Ceram. 14, 100365 https://doi.org/10.1016/j.oceram.2023.100365.
Crespo-López, L., Martínez-Ramírez, A., 2023. Pomace from the wine industry as an additive in the production of traditional sustainable lightweight eco-bricks. Appl. Clay Sci. 243, 107084 https://doi.org/10.1016/j.clay.2023.107084.
Cucato, M., de Vecchi, G.P., Mozzi, P., Abbà, T., Paiero, G., Sedea, R. (Eds.), 2008. CARG Progetto. Note illustrative della Carta Geologica d'Italia alla scalla 1:50.000. Foglio 147. Padova Sud., Istituto Superiore per la Protezione e la Ricerca Ambientale (ISPRA): Regione del Veneto, Italia.
Cultrone, G., Molina, E., Arizzi, A., 2014. The combined use of petrographic, chemical and physical techniques to define the technological features of Iberian ceramics from the Canto Tortoso area (Granada, Spain). Ceram. Int. 40, 10803–10816. https://doi.org/10.1016/j.ceramint.2014.03.072.
Cultrone, G., Sebastián, E., 2009. Fly ash addition in clayey materials to improve the quality of solid bricks. Constr. Build. Mater. 23, 1178–1184. https://doi.org/10.1016/j.conbuildmat.2008.07.001.
Cultrone, G., Rodríguez-Navarro, C., Sebastián, E., Cazalla, O., de la Torre, M.J., 2001. Carbonate and silicate phase reactions during ceramic firing. Eur. J. Mineral. 13, 621–634. https://doi.org/10.1127/0935-1221/2001/0013-0621.
Daghmehchi, M., Omrani, H., Emami, M., Nokandeh, J., 2016. Mineralogical and thermo-chemical characteristics of the Hellenistic ceramics and raw clay from Qizlar Qal'eh (northeastern Iran). Mater. Charact. 120, 143–151. https://doi.org/10.1016/j.matchar.2016.08.030.
Dalkılıç, N., Nabikoğlu, A., 2017. Traditional manufacturing of clay brick used in the historical buildings of Diyarbakir (Turkey). Front. Archit. Res. 6 (3), 346–359. https://doi.org/10.1016/j.foar.2017.06.003.
Domínguez, E.A., Ullmann, R., 1996. "Ecological bricks" made with clays and steel dust pollutants. Appl. Clay. Sci. 11, 237–249. https://doi.org/10.1016/S0169-1317(96)00020-8.
Duminuco, P., Messiga, B., Riccardi, M.P., 1998. Firing process of natural clays. Some microtextures and related phase compositions. Thermochimi. Acta 321 (1–2), 185–190. https://doi.org/10.1016/S0040-6031(98)00458-4.
Elías, M.L., Cultrone, G., 2019. On the use of sodium chloride and calcined diatomite sludge as additives to improve the engineering properties of bricks made with a clay earth from Jun (Granada, Spain). Minerals 9 (1), 64. https://doi.org/10.3390/min9010064.
Fabbri, B., Gualtieri, S., Shoval, S., 2014. The presence of calcite in archaeological ceramics. J. Eur. Ceram. Soc. 34, 1899–1911. https://doi.org/10.1016/j.jeurceramsoc.2014.01.007.
Flores, V., Guiraúm, A., Barrios, J., 1999. Caracterización de ladrillería tradicional producida en la Vega del Guadalquivir, en zonas próximas a Sevilla. Bol. Soc. Esp. Cerám. Vidrio 38 (1), 29–34.
Germinario, L., Zara, A., Maritan, L., Bonetto, J., Hanchar, J.M., Sassi, R., Siegesmund, S., Mazzoli, C., 2018. Tracking trachyte on the Roman routes: Provenance study of Roman infrastructure and insights into ancient trades in Northern Italy. Geoarchaeology 33, 417–429. https://doi.org/10.1002/gea.21667.
Gloria, A. (Ed.), 1873. Statuti Del Comune Di Padova Dal Secolo XII Al 1285. Premiata Tipografia F. Sacchetto, Padova.
Govindaraju, K., 1994. Compilation of working values and sample description for 383 geostandards. Geostandard. Newsl. 18, 1–158. https://doi.org/10.1046/j.1365-2494.1998.53202081.x-i1.
Grifa, C., Germinario, C., De Bonis, A., Mercurio, M., Izzo, F., Pepe, F., Bareschino, P., Cucciniello, C., Monetti, V., Morra, V., Cappelletti, P., Cultrone, G., Langella, A., 2017. Traditional brick productions in Madagascar: From raw material processing to firing technology. Appl. Clay. Sci. 150, 252–266. https://doi.org/10.1016/j.clay.2017.09.033.
Hein, A., Day, P.M., Quinn, P.S., Kilikoglou, V., 2004. The geochemical diversity of Neogene clay deposits in Crete and its implications for provenance studies of Minoan pottery. Archaeometry 46 (3), 7–384. https://doi.org/10.1111/j.1475-4754.2004.00163.x.
Hubbard, C., Snyder, R., 1988. RIR - Measurement and Use in Quantitative XRD. Powder Diffr. 3 (2), 74–77. https://doi.org/10.1017/S0885715600013257.
Iordanidis, A., García-Guinea, J., Karamitrou-Mentessidic, G., 2009. Analytical study of ancient pottery from the archaeological site of Aiani, northern Greece. Mater. Charact. 60, 292–302. https://doi.org/10.1016/j.matchar.2008.08.001.
Jain, L.C., Gopal, R., Jain, S.K., 1976. Lime blowing in bricks. Bâtim. Int. Build. Res. Pract. 4 (1), 48. https://doi.org/10.1080/09613217608550450.
Jobstraibitzer, P., Malesani, P., 1973. I sedimenti dei fiumi veneti. Mem. Soc. Geo. Ital. 12, 411–452.
Kingery, W.D., Vandiever, P.M., 1986. Ceramic Masterpieces. Art, Structure and Technology. The Free Press, New York.
Klaarenbeek, W., 1961. The development of yellow calcareous bricks. Trans. Br. Ceram. Soc. 60, 738–772.
Laird, R.T., Worchester, M., 1956. The inhibiting of lime blowing. Brit. Ceram. t. 55, 545–563.
Lourenço, P.B., Fernandes, F.M., Castro, F., 2010. Handmade clay bricks: chemical, physical and mechanical properties. Int. J. Archit. Heritage 4 (1), 38–58. https://doi.org/10.1080/15583050902871092.
Maritan, L., 2004. Archaeometric study of Etruscan-Padan type pottery from the Veneto region: Petrographic, mineralogical and geochemical-physical characterization. Eu. J. Mineral. 16, 297–307. https://doi.org/10.1127/0935-1221/2004/0016-0297.
Maritan, L., 2020. Ceramic abandonment. How to recognize post-depositional transformations. Archaeol. Anthropol. Sci. 12, 199. https://doi.org/10.1007/s12520-020-01141-y.
Maritan, L., Nodari, L., Mazzoli, C., Milano, A., Russo, U., 2006. Influence of firing conditions on ceramic products: Experimental study on clay rich in organic matter. Appl. Clay Sci. 31, 1–15. https://doi.org/10.1016/j.clay.2005.08.007.
Maritan, L., Ganzarolli, G., Antonelli, F., Rigo, M., Kapatza, A., Bajnok, K., Coletti, C., Mazzoli, C., Lazzarini, L., Vedovetto, P., Chavarría, A., 2021. What kind of calcite? Disclosing the origin of sparry calcite temper in ancient ceramics. J. Archaeol. Sci. 129, 105358 https://doi.org/10.1016/j.jas.2021.105358.
Maritan, L., Gravagna, E., Cavazzini, G., Zerboni, A., Mazzoli, C., Grifa, C., Mercurio, M., Ali Mohamed, A., Usai, D., Salvatori, S., 2023. Nile clayey materials in Sudan: chemical and isotope analysis as reference data for pottery provenance studies. Quat. Int. 657, 50–66. https://doi.org/10.1016/j.quaint.2021.05.009.
Mazzi, G., Verdi, A., Dal Piaz, V., 2002. Le mura di Padova. Il Poligrafo Editore, Padova.
Mozzi, P., Bini, C., Zilocchi, L., Becattini, R., Mariotti Lippi, M., 2003. Stratigraphy, palaeopedology and palynology of Late Pleistocene and Holocene deposits in the landward sector of the Lagoon of Venice (Italy), in relation to the Caranto Level, Il Quaternario. Italian Journal of Quaternary Sciences, 16, 1Bis, 193–210.
Pavia, S., 2006. The determination of bricks provenance and technology using analytical techniques from the physical sciences. Archaeometry 48, 201–218. https://doi.org/10.1111/j.1475-4754.2006.00251.x.
Pérez-Monserrat, E.M., Maritan, L., Garbin, E., Cultrone, G., 2021. Production Technologies of Ancient Bricks from Padua, Italy: Changing Colors and Resistance over Time. Minerals 11, 744. https://doi.org/10.3390/min11070744.
Pérez-Monserrat, E.M., Causarano, M.A., Maritan, L., Chavarría, A., Brogiolo, G.P., Cultrone, G., 2022a. Roman brick production technologies in Padua (Northern Italy) along the Late Antiquity and Medieval times: Durable bricks on high humid environs. J. Cult. Herit. 54, 12–20. https://doi.org/10.1016/j.culher.2022.01.007.
Pérez-Monserrat, E.M., Maritan, L., Cultrone, G., 2022b. Firing and post-firing dynamics of Mg- and Ca-rich bricks used in the built heritage of the city of Padua (northeastern Italy). Eur. J. Mineral. 34, 301–319. https://doi.org/10.5194/ejm-34-301-2022.
Piccoli, G., Sedea, R., Bellati, R., Di Lallo, E., Medizza, F., Girardi, A., De Pieri, R., De Vecchi, G.P., Gregnanin, A., Piccirillo, E.M., Norinelli, A., Dal Prà, A., 1981. Note illustrative della Carta geologica dei Colli Euganei alla scala 1:25.000. II Edizione. Mem. Sci. Geol. 34, 523–566, 1 map.
Ramos Gavilán, A.B., Rodríguez Esteban, M.A., Antón Iglesias, M.N., Sáez Pérez, M.P., Camino Olea, M.S., Caballero Valdizan, J., 2018. Experimental study of the mechanical behaviour of bricks from 19th and 20th century buildings in the province of Zamora (Spain). Infrastructures 3 (3), 38. https://doi.org/10.3390/infrastructures3030038.
Rathossi, C., Pontikes, Y., 2010. Effect of firing temperature and atmosphere on ceramics made of NW Peloponnese clay sediments. Part I: Reaction paths, crystalline phases, microstructure and colour. J. Eur. Ceram. Soc. 30, 1841–1851. https://doi.org/10.1016/j.jeurceramsoc.2010.02.002.
Riccardi, M.P., Messiga, B., Duminuco, P., 1999. An approach to the dynamics of clay firing. Appl. Clay. Sci. 15, 393–409. https://doi.org/10.1016/S0169-1317(99)00032-0.
Rodríguez-Navarro, C., Kudlacz, K., Ruíz-Agudo, E., 2012. The mechanism of thermal decomposition of dolomite: New insights from 2D-XRD and TEM analyses. Am. Mineral. 97, 38–51. https://doi.org/10.2138/am.2011.3813.
Sáenz, N., Sebastián, E., Cultrone, G., 2019. Analysis of tempered bricks: From raw materials and additives to fired bricks for use in construction and heritage conservation. Eur. J. Mineral. 31, 301–312. https://doi.org/10.1127/ejm/2019/0031-2832.
Sangiorgio, V., Parisi, F., Fieni, F., Parisi, N., 2022. The New Boundaries of 3D-Printed Clay Bricks Design: Printability of Complex Internal Geometries. Sustainability 14, 598. https://doi.org/10.3390/su14020598.
Trindade, M.J., Dias, M.I., Coroado, J., Rocha, F., 2009. Mineralogical transformations of calcareous rich clays with firing: A comparative study between calcite and dolomite rich clays from Algarve. Portugal. Appl. Clay Sci. 42, 345–355. https://doi.org/10.1016/j.clay.2008.02.008.
Vedder, W., Wilkins, R.W.T., 1969. Dehydroxylation and rehydroxylation, oxidation and reduction of mica. Am. Miner. 54 (3–4), 482–509.

Warr, L.N., 2021. IMA-CNMNC Approved mineral symbols. Mineral. Mag. 85, 291–320. https://doi.org/10.1180/mgm.2021.43.
Webb, T.L., 1952. Chemical aspects of the unsoundness and plasticity in building limes. South African Ind. Chemist. 290–294.
Wolff, P.M, Visser, J.W., 1964. Absolute intensities, Rep. 641.109. Technische Physische Dienst. Delft.